Supporting Information

Oxygen-mediated selection of Cu crystallographic orientation for growth of single-crystalline graphene

Hyeong-ku Jo[a,b,c], Hanjin Park[d], Hyung-June Lee[d], Garam Bae[b], Da Som Song[b], Ki Kang Kim[c], Wooseok Song[b*], Cheolho Jeon[e], Ki-Seok An[b], Young-Kyun Kwon[d,f*], Chong-Yun Park[a*]

[a]*Department of Physics, Sungkyunkwan University, Suwon 16419, Republic of Korea*

[b]*Thin Film Materials Research Center, Korea Research Institute of Chemical Technology, Daejeon 34114, Republic of Korea*

[c]*Department of Energy Science, Sungkyunkwan University, Suwon 16419, Republic of Korea*

[d]*Department of Physics, Kyung Hee University, Seoul 02447, Republic of Korea*

[e]*Advanced Nano Surface Research Group, Korea Basic Science Institute, Daejeon 34133, Republic of Korea*

[f]*Department of Information Display and Research Institute for Basic Sciences, Kyung Hee University, Seoul 02447, Republic of Korea*

**Corresponding authors. E-mail address:*

wssong@krict.re.kr (W. S.), ykkwon@khu.ac.kr (Y.-K. K.), and cypark@skku.edu (C.-Y. P.)

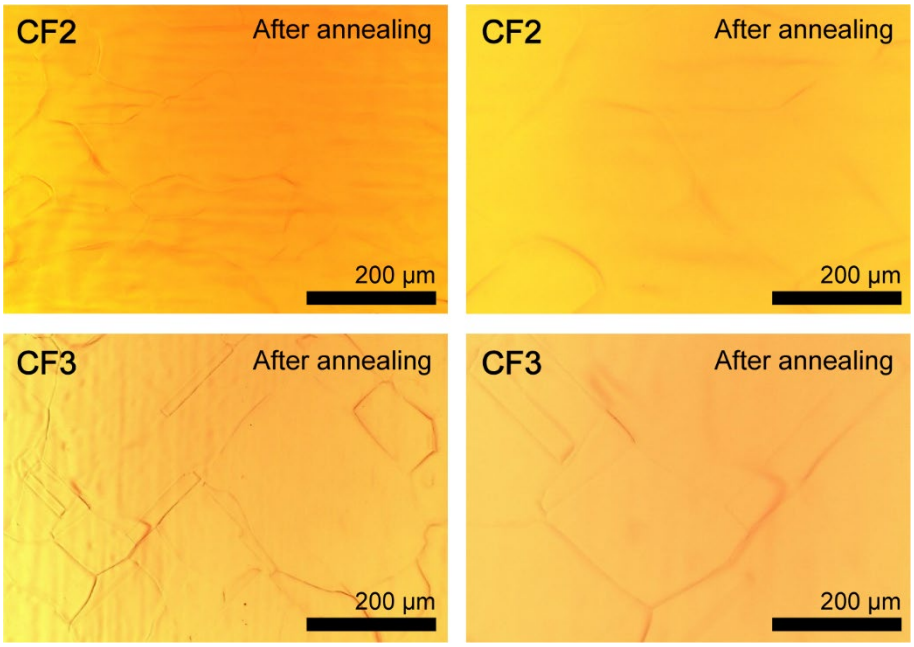

Fig. S1. Representative optical microscope images of groove evolution of CF2 and CF3 after annealing with 225 sccm H_2 at 1050 ºC for 2 h.

Note S1. Monte Carlo simulations for cyclic heat treatment

To understand the groove filling and widening processes experimentally observed during cyclic heat treatment (CHT), we performed Monte Carlo (MC) simulations based on density functional theory (DFT) calculation. To find the reaching rate of Cu adatoms to any groove edges, we first calculated the minimum energy path of a Cu adatom migrating from an fcc adsorption site to an hcp site on a Cu (111) surface as shown in Fig. 4(a). Since the binding energy of the Cu adatom on the fcc site is almost the same that on the hcp site, then we used $E_m = 76$ meV as the migration energy barrier of the Cu adatom in the Boltzmann factor corresponding to the hopping probability, $P_h = e^{-E_m/k_BT}$. With this probability, we performed MC simulations of Cu adatom diffusion on various Cu (111) domains, the sizes of which were extracted from the optical microscope image shown in Fig. 3(f). For each given sized Cu (111) domain, we counted the number of hopping trials N_t until the Cu adatom reached any edge of the domain corresponding to the groove edge in every MC run. The larger the N_t value, the lower the reaching probability, which can be given as $P_s = \langle N_t^{-1} \rangle$, where $\langle \cdots \rangle$ denotes ensemble average. Note that for ensemble average we performed MC runs $N(R) = (R/1\text{Å})^2$ times for each domain with its radius of R, for example, we ran MC runs 250,000 times for a domain with $R = 50$ nm. We also evaluated the attempt frequency f_s for the Cu adatom to hop from one adsorption site to a neighboring site by the harmonic approximation of the total energy near the equilibrium position of the adsorption site. With these two quantities as well as the area density σ of Cu adatoms and the total surface area A of the Cu (111) surface, we were able to evaluate the number per unit time of Cu adatoms to reach any groove edges or the reaching rate ν_s by

$$\nu_s = \sigma A f_s P_s. \tag{S1}$$

Then, to find the escaping rate of dangling Cu atoms at any groove edges, we similarly calculated the minimum energy path of a Cu atom migration from an edge binding site of a groove toward nearby adsorption sites on a Cu (111) surface as shown in Fig. 4(b), in which the escaping energy barrier was estimated to be $E_e = 0.96$ eV. The escaping probability P_e is simply given by the Boltzmann factor as $P_e = e^{-E_e/k_BT}$. Its attempt frequency f_e was also estimated for the Cu adatom to escape from the edge binding site to a neighboring surface site by the harmonic approximation of the total energy near the equilibrium position of the binding edge sited site. With all these quantities, thus, we were able to estimate the number per unit time of dangling Cu atoms at any groove edges to escape from their corresponding edges or the escaping rate ν_e by

$$\nu_e = \lambda L f_e P_e, \tag{S2}$$

where λ is the line density of Cu atoms at any groove edges and L is the total length of groove edges.

Fig. 4(c) shows the two linear relations between σ and λ for $\nu_s = \nu_e$ at T = 800 (blue line) and 1050°C (red line) indicating the dynamic equilibria at the respective temperatures. It is noted that, in real CHT experiments, the equilibrium relation between σ and λ should depend *dynamically* on all the variables involved in Eqs. (S1) and (S2), which would be intercoupled to one another during CHT processes. Thus, more sophisticated simulation is required for more realistic simulations. Nevertheless, our interpretation for CHT process, which was based on fixed values of σ, λ, A, L, E_m, and E_e for simplicity, still provide a basic understanding on CHT process.

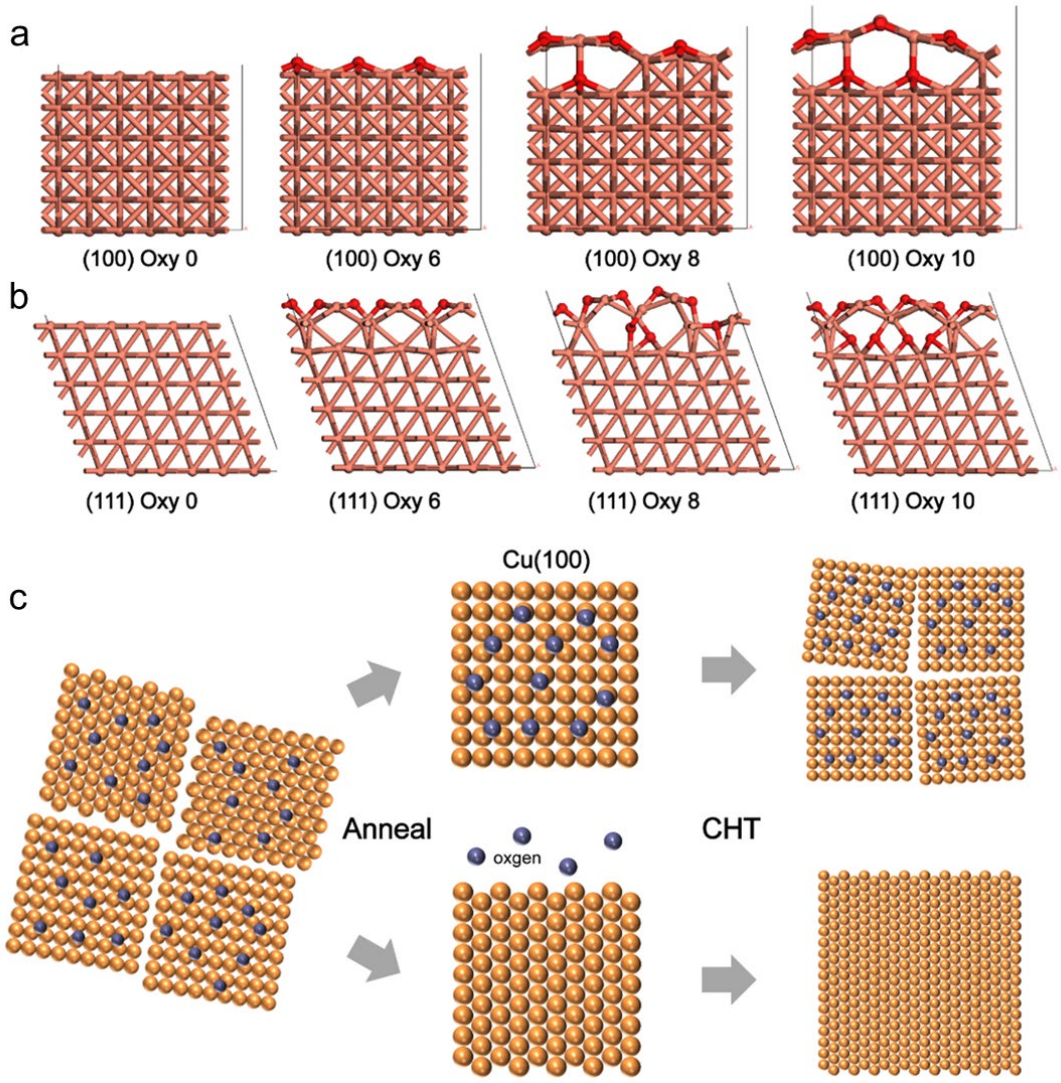

Fig. S2. Ball and stick model for atomic configuration of (a) O/Cu(100) and (b) O/Cu(111) according to oxygen coverage (red: oxygen atoms, orange: Cu atoms). (c) Schematic diagram of recrystallization mechanism in the preferential orientation of polycrystalline copper foils.

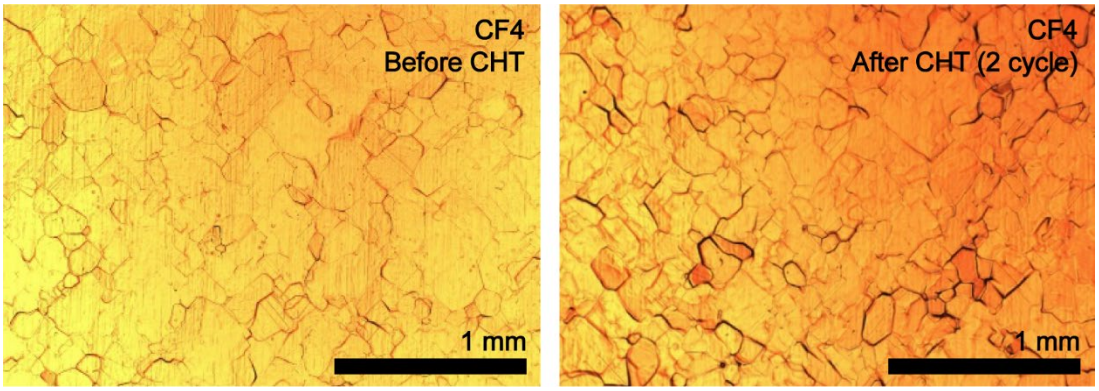

Fig. S3. Representative optical microscope images of CF4 before and after 2 cycles CHT.

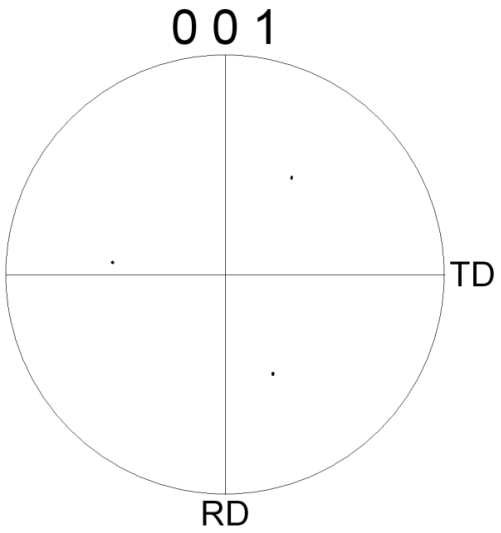

Fig. S4. Transverse direction (TD) and rolling direction (RD) maps acquired from EBSD of single-crystalline CF3 formed by CHT.

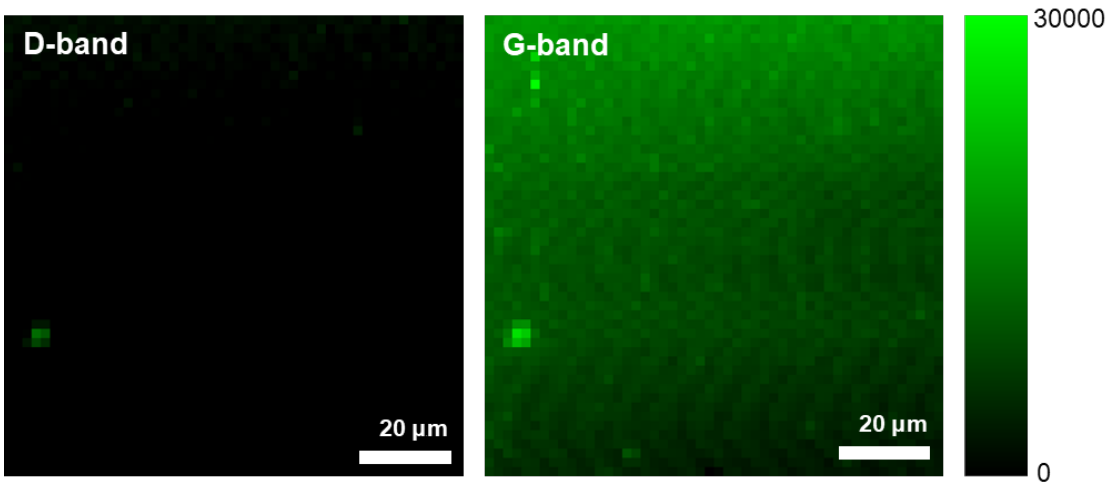

Fig. S5. The D- and G-band intensity maps of single-crystalline graphene synthesized on recrystallized CF3 (area: 100 × 100 μm^2).